High-efficiency blue generation by frequency doubling of femtosecond pulses in a thick nonlinear crystal

A. M. Weiner, A. M. Kan'an,* and D. E. Leaird

School of Electrical and Computer Engineering, Purdue University, West Lafayette, Indiana 47907-1285

Received June 9, 1998

We have demonstrated highly efficient frequency doubling of femtosecond pulses in a thick, noncritically phase-matched $KNbO_3$ crystal under conditions of large group-velocity mismatch. At low power we observed a slope efficiency of ~300% nJ^{-1} for harmonic conversion, and at higher powers we generated 170 mW of second-harmonic blue output for 300 mW of input light. Furthermore, we have shown that the focusing dependence for our conditions of large group-velocity mismatch is considerably different from that obtained for frequency doubling of continuous-wave light. We have also demonstrated that one can tune the spectral width of the generated blue light by varying the focusing conditions. © 1998 Optical Society of America

OCIS codes: 190.4160, 320.2250, 190.0190, 190.2620, 320.0320.

Generation of coherent radiation at blue and shorter wavelengths is a topic of considerable research interest. Nonlinear optical frequency conversion plays a key role in much of this research. Here we discuss a simple yet still relatively unexplored nonlinear optical approach, namely, second-harmonic generation (SHG) of femtosecond pulses by use of a thick nonlinear crystal (NLC) under conditions of large group-velocity mismatch (GVM). Using a 3-mm $KNbO_3$ crystal, we have obtained a slope efficiency of ~300% nJ^{-1} for harmonic conversion at low input powers and as much as 170 mW of second-harmonic (SH) blue output for 300 mW of input light. Although GVM in the SHG crystal broadens the output pulses into the picosecond range, our approach, coupled with rapid advances occurring in the field of femtosecond (fs) solid-state lasers, suggests the possibility of using SHG of fs pulses as an efficient means of generating blue photons for applications in which the blue-pulse duration is not critical, e.g., lithography. A key point is the use of mode-locked pulses[1,2] to provide high peak powers for enhanced nonlinear frequency conversion while avoiding the need for external enhancement cavities[3,4] and maintaining a much higher pulse repetition rate than is possible with Q-switched laser sources.[5] Furthermore, we demonstrate a novel focusing dependence and show that we can tune the spectral width of the SH light by varying the focusing conditions.

The influence of GVM on SHG was analyzed 30 years ago; plane waves, noncritical phase matching (no spatial walk-off), and no pump depletion were assumed.[6–8] The influence of GVM on fs pulse-width measurements from SHG intensity autocorrelations was also investigated.[9] Analysis[6–8] showed that GVM broadens the output SH pulse compared with the input and restricts phase matching to a narrow SH frequency range. For this reason, with a few exceptions (e.g., Refs. 2 and 10), most fs SHG experiments have used thin NLC's of the order of hundreds of micrometers or less. Here we intentionally utilize a thick crystal with large GVM and narrow phase-matching bandwidth. As a result we easily obtain high harmonic conversion efficiency, which allows us to explore SHG with strong pump depletion and large GVM simultaneously. We also investigate, for the first time to our knowledge, the focusing dependence of SHG with large GVM.

We briefly discuss the main theoretical points. We first introduce a characteristic walk-off length $l_T = t_p/\alpha$ over which the walk-off in time is equal to one pulse width t_p, where α is the GVM in picoseconds per millimeter. In the long-pulse (or cw) limit, l_T is much greater than the crystal length L ($L << l_T$); the SHG power conversion efficiency is given by the following well-known formula, assuming noncritical phase matching, low pump depletion, and weak focusing:

$$\frac{P_{2\omega}}{P_\omega} = \gamma P_\omega \frac{L^2}{b}, \quad \gamma = \frac{4{\omega_0}^2 {d_{\text{eff}}}^2}{n^2 c^3 \epsilon_0 \lambda}. \qquad (1)$$

Here $P_{2\omega}$ and P_ω are the powers at the SH and the fundamental frequency, respectively, ω_0 is the center frequency of the input pulse, d_{eff} is the effective nonlinear coefficient, $b = (2\pi {w_0}^2 n)/\lambda$ is the depth of focus, and w_0 is the beam radius at the focus. For strong focusing ($b < L$) the interaction length in the crystal reduces to approximately b, and the term (L^2/b) in Eq. (1) can be approximately replaced with b, with the result that

$$P_{2\omega}/P_\omega \cong \gamma P_\omega b\,. \qquad (2)$$

For a fixed pulse energy the conversion efficiency in the long-pulse limit depends both on the pulse width and the depth of focus. One also obtains the well-known result that for highest conversion efficiency one should optimize the focusing such that $L \approx b$.[11]

In the short-pulse limit ($l_T << L$), and assuming bandwidth-limited pulses, the conversion efficiency in the first thickness l_T of the crystal is given by Eq. (1), with l_T substituted for L.[6–8] The SHG process is essentially independent in each thickness l_T of the crystal, and therefore we obtain the total conversion efficiency by adding the efficiency in each length l_T of the NLC. As a result the conversion efficiency in

0146-9592/98/181441-03$15.00/0

terms of the SH and the fundamental pulse energies, $U_{2\omega}$ and U_ω, respectively, is approximately given by

$$\frac{U_{2\omega}}{U_\omega} = \gamma\left(\frac{U_\omega}{t_p}\right)\left(\frac{{l_T}^2}{b}\right)\left(\frac{L}{l_T}\right) = \frac{\gamma U_\omega L}{\alpha b}\,. \qquad (3)$$

We can handle stronger focusing by taking $b = [2\pi w^2(z)n]/\lambda$ in Eq. (3) to be z dependent according to the Gaussian beam formula $w^2(z) = {w_0}^2[1 + z^2/(b/2)^2]$ and then integrating over the length of the crystal. This approach is valid provided that $l_T < b$, i.e., the temporal walk-off length remains shorter than the depth of focus. The result is

$$\frac{U_{2\omega}}{U_\omega} = \frac{\gamma U_\omega l_T}{t_p}\int_{-L/2}^{L/2}\frac{\mathrm{d}z}{2\pi n w^2(z)/\lambda} = \frac{\gamma U_\omega}{\alpha}\tan^{-1}\left(\frac{L}{b}\right). \qquad (4)$$

In the limit of tight focusing ($l_T < b << L$), we obtain $U_{2\omega}/U_\omega \cong (\pi/2)(\gamma U_\omega/\alpha)$. Thus, for $l_T < b << L$, the conversion efficiency is independent of both pulse width and focusing.

We performed experiments with a mode-locked Ti:sapphire laser generating ~120-fs pulses at an 80-MHz repetition rate at 860 nm and an a-cut, 3-mm-thick $KNbO_3$ NLC that was temperature tuned for noncritical type I phase matching for SHG to 430 nm. The GVM was $\alpha = 1.2$ ps/mm,[12] which gives $l_T = 100\ \mu$m, much less than the crystal length. SHG versus input power curves were acquired over the range 3–300 mW by use of a computer-controlled variable attenuator wheel. Input infrared and output blue powers were monitored simultaneously by use of a beam splitter and a photodetector before the NLC and red blocking filters and a second photodetector after the crystal. The input beam was chopped, and both detectors were connected to lock-in amplifiers whose outputs were digitized and stored. A prism pair was used before the NLC to ensure that pump pulses from the laser were chirp free, although in practice this did not have a large effect. The input beam before the focusing lens was mildly elliptical with measured e^{-1} beam diameters of 2.2 and 2.9 mm along the horizontal and the vertical axes, respectively. Data were taken with a series of 11 lenses with focal lengths ranging from 16 to 140 mm. This resulted in calculated depths of focus (b) of 150 μm to 10 mm and L/b values from 19.5 to 0.4. Note that the values of b quoted are the average of the values computed with the beam diameter taken along either the major or the minor axis of the input beam.

Figure 1 shows SH power and efficiency versus input power for focal lengths of 31 and 140 mm. The beam is focused near the center of the NLC, which gives the highest efficiency for low input powers. The powers shown refer to the average input and blue powers while the chopper is open; the overall average powers are a factor of 2 lower owing to the 50% chopper duty cycle. We verified that the conversion efficiency at 300 mW input was unchanged when the chopper was removed. For the 31-mm lens the blue output rises sharply at first, with a low-power slope efficiency of 3.75% mW^{-1} (300% nJ^{-1}). The output power is quadratic in the input only for input powers less than 25 mW; the conversion efficiency is ~29% at 10 mW and ~46% at 25 mW, indicating significant pump depletion even at these low input powers. The highest SHG efficiency is obtained for ~50-mW average input power, above which the efficiency slowly declines. For the 140-mm lens the SH efficiency rises more slowly at first but then plateaus at higher powers, so at the highest input power more blue is generated with the longer focal-length lens. Our data demonstrate that it is remarkably easy to achieve high SH conversion efficiency with a relatively low-average-power fs laser oscillator and a thick NLC.

Figure 2 shows data on conversion efficiency versus focusing for 3.7- and 5.5-mW input powers, which are chosen to remain within the low pump-depletion regime. For tight focusing nearly 20% conversion efficiency is achieved even for only 5.5-mW input power. The relative efficiency data are in excellent agreement with Eq. (4). The absolute efficiencies are all ~3 times lower than predicted when a nonlinear coefficient $d_{\mathrm{eff}} = 20$ pm/V is used; the reason for this discrepancy is not understood. For comparison, the well-known theoretical focusing dependence expected in the long-pulse or quasi-cw limit,[11] with a clear peak at $L/b = 2.84$, is also plotted. Our data are in sharp contrast with this long-pulse result.

We also demonstrated the ability to tune the SH spectral width by focusing. Figure 3 shows the SH spectra obtained under low conversion conditions by use of three different lenses. For weak focusing the spectrum is symmetric with a width less than 0.2 nm. The spectral width increases dramatically for tighter focusing, broadening asymmetrically to the long-wavelength side. For weak focusing, phase matching is restricted to a SH bandwidth $\Delta\nu = 0.88/\alpha L$.[6] For tight focusing L should be replaced with the effective interaction length (b), and this explains the increased

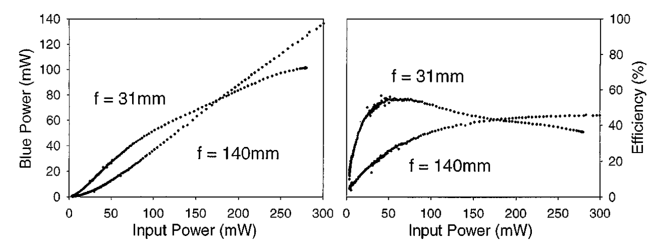

Fig. 1. SH power (left) and conversion efficiency (right) versus input power for 31- and 140-mm focal-length lenses.

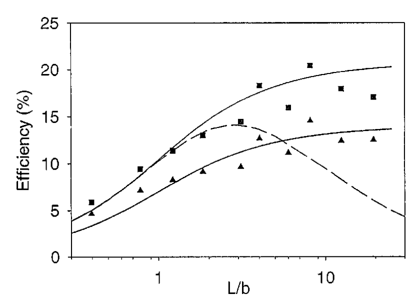

Fig. 2. SH efficiency versus focusing for 3.7-mW (▲) and 5.5-mW (■) input powers. Also shown are theoretical fits from Eq. (4) (————) and from the cw theory (– – – –).

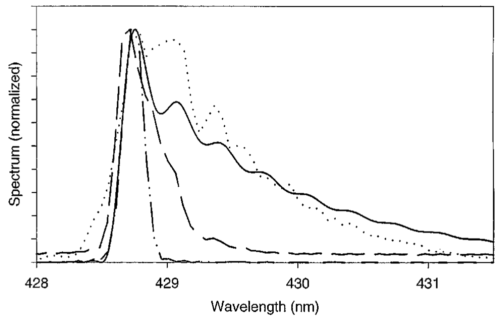

Fig. 3. SH spectra obtained for simple lenses with $f = 60$ mm(—··—··) and $f = 38$ mm (– – – –) and a 10× microscope objective ($f = 16$ mm) (·······). Also shown is the theoretical spectrum for the tightest focusing case (———).

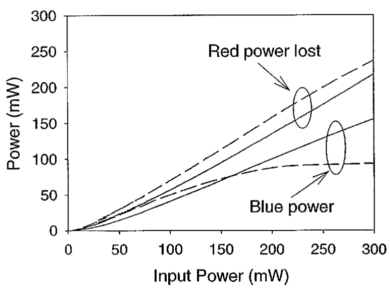

Fig. 4. SH output power and depletion in pump power for an 80-mm focal-length lens for low-power (– – – –) and high-power (———) optimizations, respectively.

spectral width. The asymmetry arises because the dispersion of $KNbO_3$ allows phase matching between two off-axis spatial frequency components of the ω wave and an on-axis component of the 2ω wave but only for one sign of phase mismatch (namely, for frequencies lower than $2\omega_0$). Similar asymmetries as a function of phase matching also arise for tightly focused Gaussian beams in cw SHG.[11] A theoretical plot of the spectrum for the tightest focusing case, computed with the cw theory, is also shown in Fig. 3, in which the phase mismatch is determined by the SH frequency offset. The theory and the data are in excellent agreement.

Finally, we investigated conversion efficiency versus the position of the focus in the NLC. For the highest input powers (~300 mW), the best SH efficiency was achieved when the focus was moved toward the back end of the crystal. Figure 4 shows SH power versus input power for an 80-mm focusing lens with foci at the center (low-power optimization) and toward the back (high-power optimization) of the NLC. Maximum SH powers of 93 and 160 mW were achieved for low- and high-power optimizations, respectively. Similar trends were found with other lenses. The highest SH power that we obtained was 173 mW, achieved at 309-mW input power with a 36-mm lens (not shown). Figure 4 also shows estimates of the pump depletion obtained by measurement of the pump power transmitted through the NLC. Clearly the depletion in pump power significantly exceeds the SH output power. This effect cannot be explained by linear loss, which is only approximately 1–2%, including reflection loss at both the pump and the SH wavelengths. By varying the crystal temperature to destroy phase matching, we verified that nonlinear absorption of the pump beam by itself is unimportant. These results suggest that nonlinear absorption of the SH light is responsible for the saturation in SH conversion efficiency at high power. Nonlinear absorption of the SH may also explain why high-power optimization occurs for focusing toward the back of the crystal; in this case the SH light passes through less material and presumably suffers less nonlinear absorption. Because SHG of fs pulses in thick NLC's results in picosecond output pulses that still have relatively high intensities, nonlinear absorption of the SH may present a fundamental barrier to achieving 100% conversion, especially (as here) for SH photons exceeding half the NLC bandgap.

In summary, we have demonstrated high-efficiency frequency doubling of fs pulses in noncritically phase-matched $KNbO_3$ under conditions of large group-velocity mismatch. At low power we observed ~300% nJ^{-1} harmonic conversion slope efficiency; at higher input power we generated 170 mW of SH blue output for 300 mW of input light. Furthermore, we demonstrated a novel focusing dependence and the ability to tune the blue spectral width by varying the focusing conditions. Similar effects may be expected for angle phase-matched SHG, although the theory must be extended to include simultaneous temporal and spatial walk-off.

We thank Greg Mizell of VLOC for the $KNbO_3$ crystal. This work was supported in part by the U.S. Air Force Office of Scientific Research and the National Science Foundation.

*Present address, Thermawave, 5950 Hazeltine National Drive, Orlando, Florida 32822.

References

1. A. Nebel and R. Beigang, Opt. Lett. **16,** 1729 (1991).
2. F. Seifert and V. Petrov, Opt. Commun. **99,** 413 (1993).
3. H. Tsuchida, Jpn. J. Appl. Phys. **33,** 6190 (1994).
4. W. J. Kozlovsky, W. Lenth, E. E. Latta, A. Moser, and G. L. Bona, Appl. Phys. Lett. **56,** 2291 (1990).
5. G. W. Ross, M. Pollnau, P. G. R. Smith, W. A. Clarkson, P. E. Britton, and D. C. Hanna, Opt. Lett. **23,** 171 (1998).
6. W. H. Glenn, IEEE J. Quantum Electron. **QE-5,** 284 (1969).
7. J. Comly and E. Garmire, Appl. Phys. Lett. **12,** 7 (1968).
8. S. A. Akhmanov, A. P. Sukhorukov, and A. S. Chirkin, Sov. Phys. JETP **28,** 748 (1969).
9. A. M. Weiner, IEEE J. Quantum Electron. **QE-19,** 1276 (1983).
10. M. A. Arbore, A. Galvanauskas, D. Harter, M. H. Chou, and M. M. Fejer, Opt. Lett. **22,** 1341 (1997).
11. G. D. Boyd and D. A. Kleinman, J. Appl. Phys. **39,** 3597 (1968).
12. B. Zysset, I. Biaggio, and P. Günter, J. Opt. Soc. Am. B **9,** 380 (1992).